International Journal of Reliability, Risk and Safety: Theory and Application

Online ISSN: 2676-3346

Vol. 8/ Issue 2/ 2025/ pp.129-137
DOI: 10.22034/IJRRS.2025.8.2.12
Received: 15 November 2025, Revised: 11 December2025, Accepted: 23 December 2025
Available online at: https://www.ijrrs.com

Original Research Article

Experimental Accuracy in Aerodynamic Blowing with High AOA for Separation Suppression

Vahid Velayati[1] and Mohammad Nadjafi[2*]

1. Department of Aerospace Engineering, Sharif University of Technology, Tehran, Iran.

2. Aerospace Research Institute, Ministry of Science, Research and Technology, Tehran, Iran

*** m.nadjafi@ari.ac.ir**

Abstract

Separation of the boundary layer on the wing can be associated with a decrease in lift and an increase in drag. This phenomenon, observed in various industries such as turbo machines, land and sea transportation, shuttles, and rockets, can have destructive effects and reduce the efficiency of the mentioned systems. It is possible to control the isolated flow with two active and passive methods. In this paper, the active method (similar gas blowing) has been used experimentally to control the flow field around the NACA0012 airfoil at a high angle of attack (18 degrees). Due to the stability of the airfoil position on the wing (about 42% of the chord with 4% of the chord width), the effect of changing the parameters of air jet blowing speed and air jet blowing angle in controlling the flow around the airfoil has been investigated. Finally, the accuracy and reliability analysis of the airfoil experimental test data was performed, and the results were obtained. Among the selected wind angles and wind speeds, the best conditions and options were introduced.

Keywords: Accuracy Analysis; Experimental Aerodynamics; High Angle of Attack; Aerodynamic Blowing; Separation Suppression.

Nomenclature and Units

D	Drag Force
E	Flow Voltage
L	Lift Force
$\frac{dp}{dx}$	Pressure Gradient
T	Temperature
u	Tangential Velocity
v	Vertical Velocity
α	Angle of Attack
ρ	Material Density
∇P	Pressure Change
δP	Amount of P error
E^2	Error Rate

1. Introduction

Boundary layer separation is a critical aerodynamic phenomenon that reduces lift and increases drag, thereby limiting aircraft performance in terms of ceiling, maneuverability, and operational range. Preventing or delaying separation is essential not only for wings and control surfaces but also for engine inlets, where separation can reduce intake efficiency and compromise propulsion systems [1]. In addition to the aerodynamic considerations that are made on the design of the body, these considerations must be taken into account in the design of the engine inlet of airplanes because the flow separation at the engine inlet reduces the air intake to the engine and, as a result, reduces the engine efficiency [2]. Among the effective factors that cause flow separation for both subsonic and supersonic flow, we can mention the limited dimensions of the surface of the object, sudden change in the geometric shape of the

How to cite this article:
V. Velayati and M. Nadjafi, "Experimental accuracy in aerodynamic blowing with high AOA for separation suppression," *International Journal of Reliability, Risk and Safety: Theory and Application*, vol. 8, no. 2, pp. 129-137, 2025, doi: 10.22034/IJRRS.2025.8.2.12.

surface of the object, viscosity, and continuous or discontinuous reverse pressure gradient [3]. Despite many theoretical studies in this field, experimental and practical studies that can express the accuracy of the data and the accuracy of the results are scarcely available. The importance of experimental studies lies in the fact that a correct understanding of the physics of the problem can be obtained, and these experiments can be used to validate the results obtained from theoretical works. Control of flow separation has been widely studied theoretically and experimentally. In the field of theory, mathematicians and physicists have attempted to derive separation control theories from the boundary layer equation, and several approximate methods for solving the boundary layer equations have been proposed [4]. The theoretical studies went towards the control of the turbulent boundary layer because the turbulent boundary layer is not separated as easily as the laminar boundary layer. However, since the region of the turbulent flow is much larger than that of the laminar flow, this delay in separation comes at the cost of increasing a certain amount of surface friction [5]. Since there was no proper understanding of turbulence in the flow, many approximate methods, which were based on semi-empirical theories, were modified to define the separation criteria of turbulent flow. In the following, experimental measurements and studies on airfoils, the effects of compressibility on the separation phenomenon, as well as analytical studies limited to simplified conditions and hypotheses, were extracted, which in most cases did not match theoretical predictions with practical results [6]. Therefore, a strong theoretical formulation was still needed to control separation, so new experimental control methods were proposed. Initially, the primary focus was on passive methods, including enhancing surface conditions (surface smoothness and curvature) and geometric shapes to delay turbulence and prevent flow separation on the upper surface of the airfoil by manipulating the pressure gradient with reduced pressure. While these methods appear to be flawless, the final answers were not entirely correct and accurate for all conditions due to the limitations of these methods in capturing the shape of the airfoil. Therefore, other passive methods were tested, such as passive suction and a passive vortex generator [7, 8].

The present study addresses this gap by experimentally investigating the flow field around a NACA0012 airfoil at a high angle of attack (18°) using surface blowing. The blowing jet was introduced at 42% chord with 4% slot width, and the effects of varying blowing speed and angle were systematically measured using a hot-wire anemometer. Unlike prior studies, this work emphasizes the accuracy and reliability of experimental data under conditions where separation is severe, thereby contributing new insights into the role of blowing parameters in controlling large separation bubbles. The novelty of this research lies in:

- Testing blowing at high angles of attack where separation is dominant.
- Using a systematic variation of blowing speed and angle to identify optimal conditions.
- Providing a detailed accuracy and reliability analysis of hot-wire measurements, ensuring that experimental data can be confidently compared with numerical predictions.

By combining experimental flow measurements with reliability analysis, this study enhances the understanding of active flow control and provides practical guidance for improving aerodynamic efficiency in aerospace applications.

2. Flow Control

Flow control becomes important when the negative effects of boundary layer separation are fully understood. With the separation of the boundary layer behind the object, a wake is created, which increases the back pressure and affects the efficiency of the system. Separation of the boundary layer in flying bodies leads to its stagnation, which decreases the drag force and increases the drag force. Another effect of the separation of the boundary layer is the Karman vortices that pass over the object with a certain frequency, which can cause the object to vibrate; if the frequency of these eddies is the same as the natural frequency of the object, it can cause the object to break. To prevent these negative effects, ways to prevent and control this phenomenon should be investigated [9].

3. Physical Concept of Flow Separation

Flow separation occurs due to adverse pressure gradients, viscosity effects, and geometric discontinuities. In the case of airfoils, separation bubbles and reverse flow regions can form, leading to turbulence and vortex shedding that degrade aerodynamic efficiency. Numerous studies have investigated methods to control separation, broadly categorized into passive and active techniques. Passive methods include vortex generators, surface modifications, and suction slots, while active methods rely on external energy input such as fluid blowing, suction, synthetic jets, and plasma actuators. Consider an inviscid region (outside the boundary layer) of fluid passing over a tapered object like the cylinder shown in **Fig. 1**. Due to the spatial limitation created by the object, the flow lines between points D and E become more compact and closer together, and then they open again at point F. Therefore, to keep the mass flow rate constant, the flow must speed up from D to E and slow down from E to F. Looking at Euler's equations (relation-1), it is clear that the effective parameter in increasing and decreasing the flow acceleration in non-viscous flow is the pressure term (∇p).

$$\rho g - \nabla P = \rho \frac{Dv}{Dt} \quad (1)$$

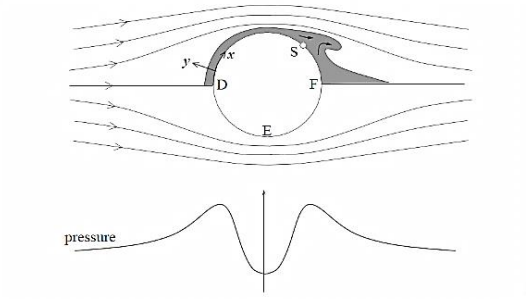

Figure 1. Pressure field and flow separation point around a cylinder

Therefore, there must be a negative (opposite) pressure gradient (dp/dx<0) to increase the fluid acceleration along the body from D to E and a positive (opposite) pressure gradient (dp/dx>0) to decrease the acceleration from E to F. In fact, the potential energy in the pressure field has been converted into kinetic energy between D and E, and then from E to F, it has completely returned to the form of potential energy because there is no source of energy loss in the inviscid fluid. Therefore, the pressure change in the x direction inside the boundary layer should be similar to the predicted results using the inviscid theory for its changes outside the boundary layer (in other words, it can be said that the outside layer strongly influences the pressure inside the boundary layer). **Fig. 2** shows the process of separating the boundary layer from the surface. As it is clear from the figure, until reaching the position of maximum thickness on the object, the desired pressure gradient (dp/dx<0) dominates the flow, but after passing this point, the reverse pressure gradient (dp/dx>0) with the opposition to the flow leads to the separation of the flow downstream. After the separation point, regions with reverse flow direction (vortices) appear.

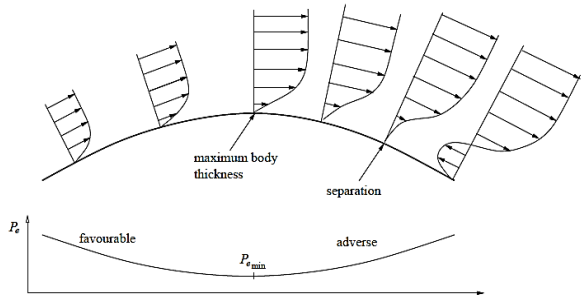

Figure 2. Separation of the boundary layer on an object

The purpose of flow control is to try to manipulate a special flow field by spending limited energy to increase the lift force and decrease the drag force. This is achieved by increasing the momentum energy and reducing the noise caused by the flow.

Examples of these techniques that produce these outputs include delaying or advancing the transition zone (from a laminar to a turbulent one), preventing or promoting separation, and stopping or increasing the disturbance. The effective factors that cause flow separation for both subsonic and supersonic flow can be mentioned as geometric issues (such as the limited dimensions of the surface of the object and sudden changes in the appearance of the object), effects of viscosity, and reverse pressure gradient. Flow control methods can be categorized into passive and active types, based on the energy consumption and cycles involved in control [10-13]. Passive control does not require the expenditure of external energy and has been widely studied [14]. Over the past few decades, researchers have focused on the development of active control methods, in which external energies such as fluid suction and blowing are introduced into the flow field [12].

4. Wind Tunnel and Instrumentation

Experimental investigations have demonstrated the effectiveness of blowing and suction in delaying stall and improving lift-to-drag ratios. For example, Greenblatt and Wygnanski showed that steady and unsteady blowing can significantly reduce separation on airfoils. Seifert et al. explored synthetic jet actuators for separation control, while Amitay et al. investigated localized blowing near the leading edge. More recent work has examined plasma actuators and hybrid methods combining passive and active devices. Despite extensive research, most studies focus on moderate angles of attack or specific Reynolds numbers, leaving gaps in understanding the effectiveness of blowing at high angles of attack. In experimental methods, models, test equipment, and measuring devices are required and are typically more expensive than those used in numerical methods. Considering the challenges of measuring certain quantities of fluid flow or unsteady flows over very short times, such as tracking the flow around an aerodynamic object from zero moment to the time of boundary layer formation, the use of methods is complicated. In numerical methods, the governing equations of fluid flow are solved by different methods. In these methods, due to the simplification of the equations governing the fluid flow, the error caused by the turbulence model, or the influence of the boundary conditions, there is a possibility of error in the obtained results. It is better to compare the accuracy of the results with the results of the method [15-16]. Compared the experimental results and modified the written program [17-18]. According to current research, it is more effective to use both numerical and experimental methods in a complementary manner. The wind tunnel creates a controlled airflow that passes around the desired model and simulates the real conditions on a smaller scale. By using tunnel accessories, the necessary information about how the airflow passes around the model is obtained, making it one of the best and most

cost-effective experimental methods for research in the field of aerodynamics.

The hot wire flow meter is a tool that can measure the instantaneous velocity of the fluid flow with high frequency, and using the measured instantaneous velocity, the average velocity, fluid flow disturbances, and tension [19]. It measured the Reynolds number, flow angle (if a two-dimensional or three-dimensional hot wire was used), flow temperature, and flow direction (especially in reverse flows). The basis of the operation of the hot wire flow meter is the transfer of heat from a wire with a very small diameter (about a few micrometers) made of tungsten, platinum, or platinum alloys. This hot wire is installed on two bases and placed in the path of fluid flow. Any change in the fluid flow conditions affects the heat transfer rate from the wire, which is determined by the hot wire flow meter. When the speed of the fluid flow decreases, the sensitivity of other methods to the change of flow conditions decreases, but the sensitivity of the hot wire flow meter increases with the decrease in speed. Therefore, it is better to use a hot wire flow meter to measure and study fluid flow at low speeds. To calibrate the hot wire flow meter, first determine the speed range and divide it into at least 10 parts. Then, calibrate the device at these points. An important point in performing the calibration process is that the conditions of the probe during calibration and testing must be the same. Due to the high sensitivity and accuracy of the hot wire flow meter device, it is better to use the same calibrator device to avoid errors. In other words, it is better not to change the place and conditions of calibration and testing.

The design and construction of the probe transfer mechanism is not a problem for the wind tunnel, which has a cross-section of the test section larger than 1.5 square meters, and it can be placed inside the test section. But for wind tunnels similar to the one used in this research, where the cross-sectional area of the test section is small due to the increase in the blocking ratio of the tunnel (the ratio of the cross-sectional area closed by the model and the rest of the equipment inside the test section to its open cross-sectional area), it is not The mechanism can be installed in the test section, and it should be placed outside the test section (**Fig. 3**).

Experiments were conducted in a closed-circuit subsonic wind tunnel with a rectangular test section. The free-stream velocity was set to 16.5 m/s, corresponding to a Reynolds number based on chord length of approximately 2.0×10^5. Flow measurements were obtained using a calibrated hot-wire anemometer (tungsten probe, diameter ≈ approximately 5 μm), capable of resolving instantaneous velocity fluctuations and mean profiles. Calibration was performed at ten discrete velocity points, ensuring consistency between calibration and test conditions.

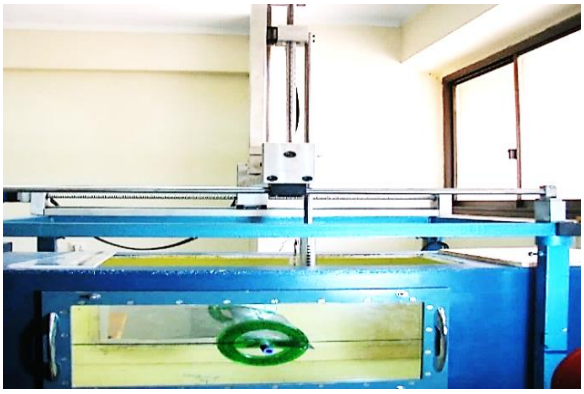

Figure 3. Probe transfer mechanism outside the test chamber

5. Airfoil Model and Blowing System

While a model is placed in a closed test chamber of a wind tunnel, it blocks the flow through this chamber. This blockage can lead to an increase in the velocity of the transmembrane fluid over the model. If the dimensions of the model are not too large compared to the dimensions of the tunnel test chamber, this speed increase is insignificant. It is constant in almost all parts of the model, and the fluid flow passing through the model can be assumed to be uniform. Therefore, the dimensions of the airfoil model used in the wind tunnel are determined according to the amount of obstruction created by the model in the tunnel. The amount of blockage in the wind tunnel is defined as the ratio of the cross-sectional area occupied by the model to the cross-sectional area of the wind tunnel test chamber. Plexiglas was used to make the model. At first, airfoils with NACA0012 airfoil coordinates and a chord size of 12 cm were prepared by using thin pile sheets (thickness 1 mm). Then, according to the location of the rotation axis of the wing cross-section, a hole with a diameter of one centimeter was created in the place of the greatest thickness on all the stencils. Since it was necessary to conduct the air into the wing cross-section to conduct the flow research, a pipe made of pilex with a diameter of 1 cm and a length of 50 cm was passed through these openings, which, in addition to delivering air to the entire wing and acting as the axis of the wing cross-section It can also be used to install wings on the side walls of the wind tunnel. After passing the tube through the opening created in the airfoils, they were placed so that the distance between the first airfoil and the last airfoil was 40 cm (the size of the opening of the wing section). To strengthen the structure, in addition to this pipe, the trailing edges of the templates were also connected with Pilex blades. The airfoil manufacturing steps are shown in **Fig. 4**, and the section of the wing installed inside the test chamber is shown in **Fig. 5**.

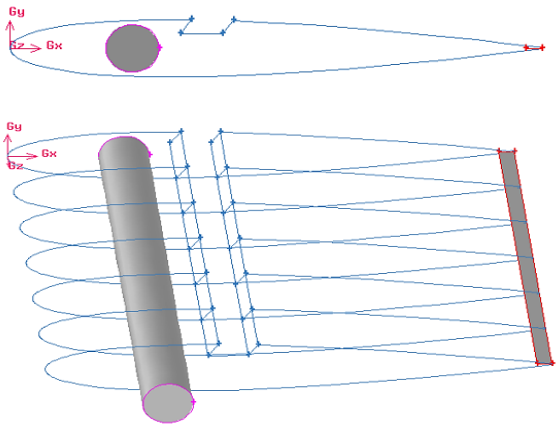

Figure 4. Design and construction of the initial structure of the wing section

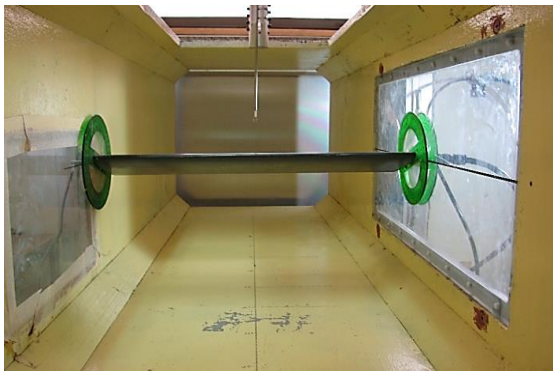

Figure 5. View of the wing section installed and the hot wire sensor inside the test chamber

This research aims to optimize the aerodynamics of the NACA0012 airfoil at a high angle of attack (18 degrees) using air blowing. When the airfoil is placed at an angle of attack of 18 degrees, a significant portion of its upper surface undergoes flow separation, which has a negative impact on the wing's performance and efficiency. To control and mitigate this phenomenon, this article employs the method of blowing air onto the wing. Effective parameters in this method can be the tail position, injection angle, and tail speed. In this article, the blowing position is placed at 42% chord with 4% chord width, the free flow speed is 16.5 m/s, and the optimal blowing speed is considered 30 m/s.

At first, considering the speed of the airfoil as fixed, the angle of the airfoil is set at three angles of 15 degrees, 20 degrees, and 25 degrees with respect to the chord, and the velocity field on the airfoil and its wake is measured using a hot wire flow meter. After performing these tests, by comparing the results, the effect of changing the injection angle on the flow control on the wing is checked, and the optimal injection angle is obtained. In the next step, the angle of the tail remains constant, and the speed of the tail is changed. Therefore, the effect of changing the gust speed at an injection angle on the flow field is investigated. Finally, a combination of gust position, gust speed, and injection angle is achieved to eliminate the vortices formed on the wing completely, thereby enhancing the aerodynamic characteristics. According to these settings, the velocity components in the upstream and downstream regions of the flow were measured using a hot-wire sensor. The results of this measurement are presented in Figs. 6 and **7**.

The test article was a NACA0012 airfoil with a chord length of 0.12 m and a span of 0.40 m, constructed from Plexiglas. A blowing slot was integrated at 42% of the chord length on the upper surface, with a slot width of 4% of the chord. A cylindrical plenum and supply tube (diameter 1 cm, length 50 cm) delivered compressed air to the slot. The blowing jet was aligned with the local surface tangent, and its angle relative to the chord could be varied.

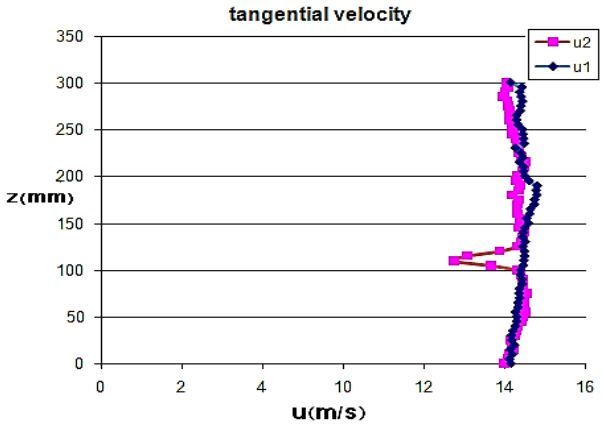

Figure 6. Profiles of the tangential component of the velocity upstream and downstream of the airfoil

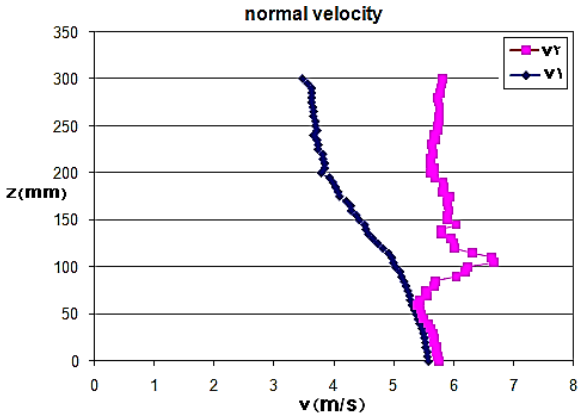

Figure 7. Profiles of the vertical component of the velocity upstream and downstream of the airfoil

6. Blowing Parameters

Two sets of parametric studies were performed:

- Blowing angle variation: 15°, 20°, and 25° relative to the chord line.
- Blowing speed variation: 20 m/s, 30 m/s, and 35 m/s.

These values were chosen to investigate the sensitivity of separation control to both injection angle and jet momentum ratio. The baseline case (no blowing) was also measured for comparison.

7. Measurement Procedure

Velocity profiles were recorded upstream, over the airfoil surface, and in the wake region. Both tangential (u) and vertical (v) velocity components were measured at multiple chordwise stations. Lift and drag forces were derived from momentum theory and validated against Kutta–Joukowski relations. Data accuracy was assessed using uncertainty analysis based on calibration constants and measurement errors in voltage and temperature.

The hot-wire anemometer used a single-wire tungsten probe (5 µm diameter) aligned tangentially to the local flow direction. Probe orientation was adjusted using a precision gimbal mount to ensure alignment with the freestream and wake flow vectors. Temperature drift was monitored using a reference thermocouple placed near the test section, and calibration was repeated every 30 minutes to mitigate thermal drift. Uncertainty propagation followed a step-by-step approach: (1) determine voltage and temperature uncertainties, (2) apply calibration curve derivatives, (3) compute propagated uncertainty in velocity, (4) propagate into force and coefficient calculations using momentum theory equations.

8. Validation

To ensure physical consistency, baseline tunnel flow was compared with reference velocity distributions. The corrected profiles confirmed that vertical velocity components approach zero far from the airfoil, as expected. This validation step addresses concerns about unrealistic velocity values in earlier plots.

By assuming constant pressure in the test chamber, the axial and normal forces are obtained using the momentum theory as follows:

$$\begin{aligned} \mathrm{F(A)} &= \int \rho u_2(u_1 - u_2)dy \\ \mathrm{F(N)} &= \int \rho(u_2 v_2 - u_1 v_1)dy \end{aligned} \quad (2)$$

In these relationships, index 1 is related to upstream, and index 2 is related to downstream. If the Kutta-Joukowski theory is used, these relationships are as follows:

$$\begin{aligned} \mathrm{F(A)} &= \int \rho U_\infty(u_1 - u_2)dy \\ \mathrm{F(N)} &= \int \rho U_\infty(v_2 - v_1)dy \end{aligned} \quad (3)$$

According to the measured values and relationships 2 and 3, axial and vertical forces are obtained. Equation 4 was used to depict these forces in the direction of the lift force and drag force.

$$\begin{aligned} L &= \mathrm{F(A)}\sin(\alpha) + \mathrm{F(N)}\cos(\alpha) \\ D &= \mathrm{F(A)}\cos(\alpha) - \mathrm{F(N)}\sin(\alpha) \end{aligned} \quad (4)$$

Finally, after getting the drag force and the drag force, using equation 5, the drag and drag coefficients are obtained:

$$\begin{aligned} C_l &= \frac{L}{\left(\frac{1}{2}\rho {U_\infty}^2 c\right)} \\ C_d &= \frac{D}{\left(\frac{1}{2}\rho {U_\infty}^2 c\right)} \end{aligned} \quad (5)$$

Table 1 compares the accuracy of these values with the results obtained from numerical research and experimental methods. According to the applied approximations, the results obtained from this measurement are comparable with the existing numerical and experimental results, indicating that the model is built with good accuracy and the measuring device has acceptable accuracy. **Fig. 8** shows the average speed profiles of the main component of the speed as a function of the dimensionless vertical distance in different positions from the leading edge to the trailing edge.

To strengthen validation, RMSE and relative error metrics were computed by comparing measured velocity profiles with benchmark NACA0012 datasets at 18° AOA. The RMSE between experimental and reference profiles was 0.42 m/s, and the relative error remained below 6% across most chordwise locations. Tunnel blockage effects were corrected using empirical blockage correction factors based on the model-to-test-section area ratio (blockage ratio ≈ 6.4%). Corrected velocity and force values were used in all subsequent analyses.

Table 1. Comparison of the accuracy of the measured lift and drag coefficients with numerical and experimental values

Aero. Parameter	Numerical Results	Wing-section Theory	Present Research	
			Kutta	Momentum
C_l	0.465	0.35	0.422	0.382
C_d	0.007	0.025	0.034	0.031

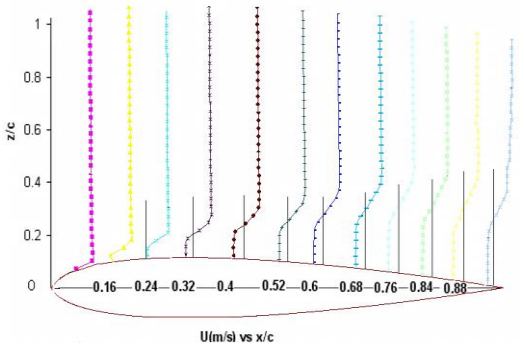

Figure 8. Average speed profiles in different airfoil positions

In **Fig. 9**, these results are drawn as speed contours. As it is clear from the figure, the separation of flow on the airfoil starts from the position of x/c=32% and extends to the tail of the airfoil.

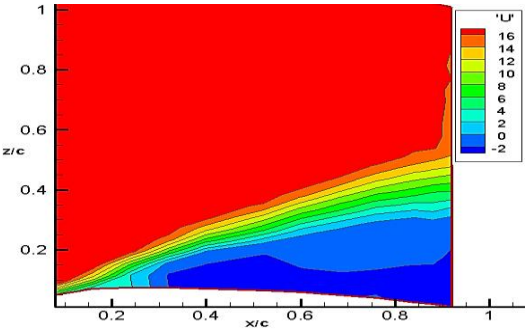

Figure 9. Average speed contour on an airfoil at an angle of attack of 18 degrees

Fig. 10 shows the reverse flow distribution on the airfoil. The separated flow region starts from about x/c=32% with the value of reverse velocity 2m/s and extends to the tail.

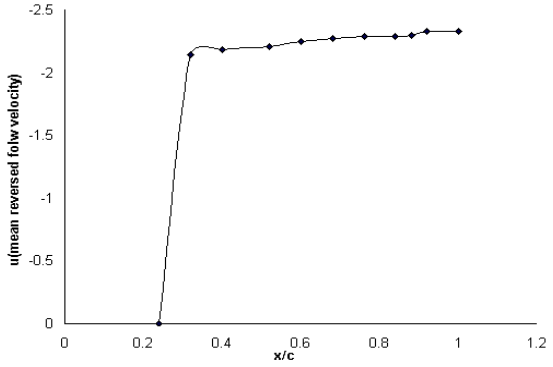

Figure 10. Average reverse flow velocity on the airfoil

In the following, the measurement range is extended from the airfoil to its trail. This measurement started from the trailing edge of the airfoil and continued until about twice the chord (the maximum distance that could be practically moved away from the airfoil). At that time, the effects of the airfoil were almost eliminated. The free flow was established again. **Fig. 11** shows the average speed profiles of the main component of the speed as a function of the dimensionless vertical distance at different positions in the airfoil trail.

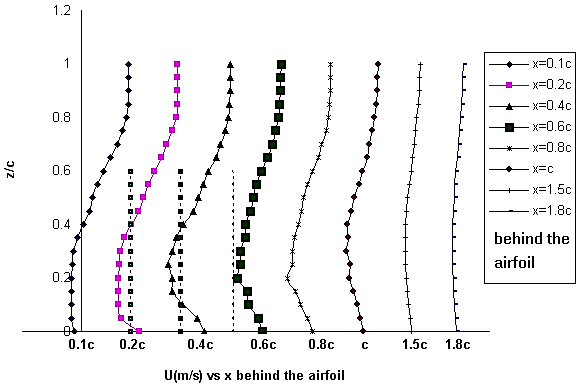

Figure 11. Average velocity profiles at positions in airfoil trail

Contours and profiles for different injection angles have been calculated and drawn. According to the experiments, the results showed that among the three blowing angles chosen to investigate the blowing effects in controlling the flow around the NACA0012 airfoil at a high angle of attack, the 15-degree blowing angle is the best choice, which is in good agreement with the results.

9. Analyzing the Accuracy and Reliability of the Results

The occurrence of human and equipment errors in experimental work seems inevitable. If these errors are not identified and controlled, the results obtained from these experiments will not be reliable. Among these errors that may occur in most practical experiments are errors related to the eye, measuring device errors, and calculation errors. However, since different factors can affect a measurement, it is very difficult and possibly impossible to accurately and definitively determine the error that occurred in the measurement. According to the mentioned cases, by using the existing methods, the measurement error can be approximately calculated by considering the effective and determining factors. In this research, the measured quantity is the average speed, and its measurement error was calculated using the Adams method [8]. Based on this method, if P is a function of the variables q, r, s, then the overall differential or overall changes in P due to partial changes δq, δr, δs is obtained in the form of the following relationship:

$$(\delta P)^2 = \left|\frac{\delta P}{\delta q}\right|^2 (\delta q)^2 + \left|\frac{\delta P}{\delta r}\right|^2 (\delta r)^2 + \left|\frac{\delta P}{\delta s}\right|^2 (\delta s)^2 \quad (6)$$

The amount of error P due to the changes in these parameters is calculated as follows:

$$\%Error = \frac{\delta P}{P} \times 100 \quad (7)$$

The variables that affect the speed in this test are the voltage and the ambient temperature. The ambient temperature is measured using the available thermometer, and the voltage value is determined from the speed calibration curve, the accuracy of which is recorded on the data card. The vector is dependent. The following relations are used to calculate the amount of error in evaluating the measured average speed:

$$\begin{aligned} U = f(E, T_\infty) \rightarrow \delta U &= \left|\frac{\delta U}{\delta E}\right| \delta E + \left|\frac{\delta U}{\delta T_\infty}\right| \delta T_\infty \\ E^2 &= (A + BU^n)(T_m - T_\infty) \\ U &= \left[\frac{1}{B}\left(\frac{E^2}{T_m - T_\infty} - A\right)\right]^{\frac{1}{n}} \end{aligned} \quad (8)$$

In the above relationships, E represents the voltage, T_∞ represents the ambient temperature equal to 27 degrees Celsius, T_m represents the temperature of the hot wire sensor equal to 250 degrees Celsius, U represents the average flow speed, and A, B, and n are the constants of the calibration relationship. According to the calibration diagram, the sensors are obtained as follows:

$$\begin{aligned} &Sensor1: A = 5.856; B = 4.696; n = 0.41 \\ &Sensor2: A = 5.4349; B = 3.4785; n = 0.6 \end{aligned} \quad (9)$$

According to the specifications of the data recording card, which is of the 12-bit type and has a voltage range of -10 to 10 volts, the accuracy of the data card voltage is approximately 5 millivolts. The accuracy of measuring the ambient temperature with the help of the thermometer is 0.5 degrees Celsius. Based on this, according to relation 7, the maximum and minimum uncertainty in speed calculation are equal to 7% and 1%, respectively. The process of uncertainty changes so that with the increase in speed, the accuracy of the measurement also increases.

To quantify the impact of measurement uncertainty on aerodynamic coefficients, the propagated uncertainty in lift (Cl) and drag (Cd) coefficients was calculated. Using the maximum and minimum velocity uncertainties

(1% to 7%), the resulting uncertainty in Cl and Cd was estimated using error propagation formulas. For example, at 7% velocity uncertainty, Cl uncertainty reached ±0.030, and Cd uncertainty reached ±0.0025. Confidence intervals (95%) were computed assuming a Gaussian error distribution. Reliability was assessed by comparing repeated measurements, yielding a standard deviation of less than 3% across trials, indicating high repeatability.

These findings have direct implications for stall risk mitigation and flight safety. By delaying separation at high AOA, the blowing system enhances lift and reduces drag, potentially extending the operational envelope of aircraft during takeoff, landing, and maneuvering. However, the implementation of active blowing systems introduces reliability concerns, including actuator degradation over time, plenum pressure fluctuations, and unsteady jet behavior. These risks must be addressed through robust actuator design, redundancy, and real-time flow monitoring to ensure consistent performance in operational settings.

10. Conclusion and Summing up

This study experimentally investigated the effect of surface blowing on flow separation control for a NACA0012 airfoil at a high angle of attack (18°). Baseline measurements confirmed extensive separation over the upper surface, with a large recirculation bubble extending from approximately 32% of the chord to the trailing edge. Systematic tests of blowing angle and speed demonstrated that jet orientation plays a critical role in energizing the boundary layer. A blowing angle of 15° at a jet speed of 30 m/s was found to be the most effective configuration, eliminating the separation bubble and restoring attached flow. Increasing the jet speed beyond 30 m/s did not yield further improvements, highlighting the importance of efficiency in active flow control. The novelty of this work lies in its focus on high-angle-of-attack conditions, where separation is severe, and in the systematic accuracy analysis of hot-wire measurements to ensure the reliability of experimental data. These results provide new insights into the role of blowing parameters in separation control and contribute to the broader understanding of active aerodynamic methods for improving lift and reducing drag. Future work should extend these experiments to different Reynolds numbers and explore hybrid control strategies combining blowing with passive devices, thereby broadening the applicability of the findings to practical aerospace systems. The obtained values were in acceptable agreement with the results of the Fluent software, confirming the accuracy of the built model. At this stage, the lift and drag force coefficients of the airfoil at the angle of attack of 4 degrees were approximately obtained, which had an acceptable accuracy compared to the existing numerical and experimental results. Then, the final tests began. These tests were performed in three stages:

- Tests without blowing
- The effect of changing the blowing angle on flow control
- The impact of changing the blowing speed on controlling the flow

In the first stage, the airfoil was installed at an angle of attack of 18 degrees, and without the effects of the wind, the velocity profiles were measured on the airfoil and its wake. The measured values showed that a wide area of the upper surface of the airfoil undergoes flow separation at this angle of attack (about 68%). The results of this stage were used as base values for the next stages, and the effects of the blowing were compared.

In the second step, the effect of changing the air jet blowing angle was investigated. At this stage, the blowing speed of the air jet was considered to be 30 m/s, and the tests were performed for three blowing angles of 25 degrees, 20 degrees, and 15 degrees with respect to the airfoil chord. The results showed that the injection angle of 25 degrees could not eliminate the reverse flow area on the airfoil, and a separation bubble remains on the airfoil at the position of about 40% of the chord, and the flow after the position of 96% of the chord. It is separated from the surface of the airfoil again and is dragged to the trail. By reducing the injection angle to 20 degrees, the results became more favorable, and the flow separation from the wing tip disappeared; however, a small bubble of backflow remained on the airfoil. Therefore, the reduction of the injection angle continued to eliminate the vortices on the wing. In this part of the tests, the blowing angle of the air jet was set to 15 degrees, the tests were performed, and the results showed that with these blowing conditions, the area of the reverse flow from the wing and its trail had been destroyed. Therefore, at this stage, the injection angle of 15 degrees provided better results than other angles. In the third step, the effect of changing the air jet blowing speed was investigated. At this stage, the angle of the air jet was set to 25 degrees. Initially, the blowing speed of the air jet was set at 20 m/s. By repeating the tests for these conditions, the results showed that a flow area separated from the wing surface remained at the position of about 40% of the chord, and the flow from the position of about 76% of the chord was separated from the wing surface again, and this separation has also continued. After this test, the tail speed was increased to 30 m/s, and the results showed that there is a separated flow bubble at the position of 40% of the chord on the wing and also at the end of the wing from about 96% of the chord of the flow again from the wing surface. It is noted that this resulted in better outcomes than before. In the continuation of the experiments of this stage, the wind speed increased to 35 m/s. The experiments were conducted under new conditions, and the results showed that there was no noticeable change in the results of the blow at a speed of 30 m/s. Therefore, it was concluded that a higher fan speed does not necessarily mean better performance, and from one speed to the next (optimal speed), increasing the speed does not result in better flow control. It is possible that by

increasing the fan speed, the instabilities caused by the blow and the eddies do not disappear completely.

Conflict of interest

No conflict of interest has been expressed by the authors.

11. References

[1] C.R. Resendiz, "Numerical Simulation of Flow Separation Control by Oscillatory Fluid Injection," Ph.D. dissertation, Texas A&M University, 2005.

[2] M. Gad-el-Hak., "Introduction to flow control," *Flow Control: Fundamentals and Practices,* M. Gad-el-Hak and A. Pollard, Eds. Berlin, Heidelberg: Springer, 1998, https://doi.org/10.1007/3-540-69672-5_1.

[3] J. Favier, A. Dauptain, and D. Basso, "Passive separation control using a self-adaptive hairy coating." *Journal of Fluid Mechanics,* vol. 627, pp. 451-483, 2009, https://doi.org/10.1017/S0022112009006119.

[4] R. Narasimha, T. S. Prahlad, and S. Ahmed, "Flow Control and Diagnostics," *Sadhana,* vol. 32, no. 1-2, pp. 1–15, 2007.

[5] R. Razaghi, N. Amanifard, and N. Narimanzadeh, "Modeling and multi objective optimization of stall control on NACA0015 airfoil with a synthetic jet using GMDH type neural networks and genetic algorithms," *International Journal of Engineering, Transactions A: Basics*, vol. 22, no. 1, pp. 69-88, 2009.

[6] I.H. Abbott and A.E. Von Doenhoff, *Theory of Wing Sections*, New York: Dover Publications, 1958.

[7] L.F. Adams, *Engineering Measurements and Instrumentation*, English University Press, Ltd, 1975.

[8] V. Kitsios, R.B. Kotapati, R. Mittal, A. Ooi, J. Soria, and D. You, "Numerical simulation of lift enhancement on a NACA 0015 airfoil using ZNMF jets," in *Proceedings of the 2006 Summer Program, Center for Turbulence Research,* pp. 457-468, Stanford, United States, 2006.

[9] K.A. Ramesh and L.V. Jose, "Active control of shock/boundary layer interaction in transonic flow over airfoils," *11th International Congress of Theoretical and Applied Mechanics*, Warsaw, Poland, 2004, pp 361–366, https://doi.org/10.1007/3-540-31801-1_50.

[10] N.K. Beliganur and P. Raymond, "Application of evolutionary algorithms to flow control optimization," *Region III AIAA Student Conference Report of University of Kentuchky*, Kentucky, USA, 2007.

[11] M.H. Shojaefard, A.R. Noorpoor, A. Avanesians, and M. Ghaffarpour, "Numerical investigation of flow control by suction and injection on a subsonic airfoil," *American Journal of Applied Sciences*, vol. 2, no. 10, pp. 1474-1480, 2005, https://doi.org/10.3844/ajassp.2005.1474.1480.

[12] P.L. Raymond, N. Beliganur, T. Hauser, "Flow control optimization using neural networks and genetic algorithms," in *4th International Conference on Computational Fluid Dynamics,* Ghent, Belgium, 2006, https://doi.org/10.1007/978-3-540-92779-2_86.

[13] S. Abdolahipour, "Review on flow separation control: Effects of excitation frequency and momentum coefficient," *Frontiers in Mechanical Engineering,* vol. 10, 2024, Art. no. 1380675, https://doi.org/10.3389/fmech.2024.1380675.

[14] S. Lee, Y. Zhao, J. Luo, J. Zou, J. Zhang, Y. Zheng, and Y. Zhang, "A review of flow control strategies for supersonic/hypersonic fluid dynamics," *Aerospace Research Communications,* vol. 2, 2024, Art. no. 13149, https://doi.org/10.3389/arc.2024.13149.

[15] M. Nadjafi and A. Najafi ARK, "Improving accuracy in importance sampling: an integrated approach with fuzzy-strata sampling," *International Journal of Reliability, Risk and Safety: Theory and Application*, vol.4, no.1, pp. 61-67, 2021, http://www.ijrrs.com/article_138602.html.

[16] M. Nadjafi, M.A. Farsi, F. Ommi, "Uncertainty analysis of spray injection process in a model-scale liquid fuel micro-motor," *Iranian Journal of Mechanical Engineering Transactions of the ISME*, vol. 21, issue 2, 2020, Art. no. e46442, https://jmee.isme.ir/article_46442.html.

[17] H. Zhang, *et al.*, "Active control of turbulent flow separation over a flapped airfoil," in *AIAA 2024 Regional Student Conferences,* 2024, Art. no. 82700, https://doi.org/10.2514/6.2024-82700.

[18] S. Norouzi, V. Velayati, S. Rostami, Kh. Javadi, and M. Taeibi-Rahni, "Physics understanding and control of boundary layer separation employing surface microstructures," *Physics of Fluids,* vol. 36, no. 7, 2024, Art. no. 075164, https://doi.org/10.1063/5.0212642.

[19] C.Y. Ma, H.Y. Xu, and C.L. Qiao, "Comparative study of two combined blowing and suction flow control methods on pitching airfoils," *Physics of Fluids*, vol. 35, no. 3, Art. no. 035120, 2023, https://doi.org/10.1063/5.0138962.